Tea tree oil nanoliposomes: optimization, characterization, and antibacterial activity against *Escherichia coli* in vitro and in vivo

RuoNan Bo,[*,†] YiWen Zhan,[*,†] SiMin Wei,[*,†] ShuYa Xu,[*,†] YinMo Huang,[*,†] MingJiang Liu,[*,†] and JinGui Li[*,†,1]

[*]*School of Veterinary Medicine, Yangzhou University, Yangzhou 225009, PR China; and* [†]*Jiangsu Co-innovation Center for Prevention and Control of Important Animal Infectious Diseases and Zoonoses, Yangzhou 225009, PR China*

ABSTRACT The purpose of this study was to formulate tee tree oil nanoliposomes (**TTONL**) and evaluate its characterization and antibacterial activity. **TTONL** was prepared by thin film hydration and sonication technique, and the preparation conditions were optimized by Box-behnken response surface method. The characterization (morphology, size, zeta potential, and stability) and antibacterial activity of TTONL against *Escherichia coli* (***E. coli***) in vitro and in vivo were evaluated. The optimal preparation conditions for TTONL: lecithin to cholesterol mass ratio of 3.7:1, TTO concentration of 0.5%, and pH of the hydration medium of 7.4, which resulted in a TTONL encapsulation rate of 80.31 ± 0.56%. TTONL was nearly spherical in shape and uniform in size, and the average particle size was 227.8 ± 25.3 nm with negative charge. The specific disappearance of the TTO peak in the infrared spectrum suggested the successful preparation of TTONL, which showed high stability at 4°C within 35 d. The result of MIC test found that the nanoliposomes improved antibacterial activity of TTO against various *E. coli* strains. TTONL exposure in vitro caused different degrees of structural damage to the *E. coli*. TTONL by oral administration alleviated the clinical symptoms and intestinal lesion of chickens induced with *E. coli* challenge. Furthermore, TTONL treatment remarkably lowered the mRNA expression of NLRP3 and NF-κB (p65) in the duodenum and cecum of *E. coli*-infected chickens. In conclusion, the prepared TTONL had good stability and slow-release property with dose-dependent inhibition and killing effects on different strains of *E. coli*, and exerted a preventive role against chicken colibacillosis through inhibition.

Key words: tea tree oil nanoliposomes, response surface methodology, antibacterial activity, chicken colibacillosis

2023 Poultry Science 102:102238
https://doi.org/10.1016/j.psj.2022.102238

INTRODUCTION

Antibiotics as feed additives are one of the effective methods to prevent and control various animal bacterial infectious diseases (Holmes et al., 2016). However, with the continuous emergence and spread of drug-resistant strains, animal bacterial infectious diseases have become an important factor that limiting the livestock industry in China (Zhao et al., 2019). Most strains of *E. coli* naturally present in the intestine are not pathogenic, but its virulent strains can cause gastroenteritis, hemorrhagic colitis, and Crohn's disease. Colibacillosis is characterized by multiorgan lesions with air sac inflammation and associated pericarditis, peri-hepatitis, and peritonitis, which initially develop in the respiratory tract and air sacs, causing considerable mortality in poultry (Lim et al., 2010). And yet, plant essential oils are expected to be developed as new antibacterial agents to alleviate the problem of antibiotic resistance because of their good antibacterial effect (Yang et al., 2021). However, many essential oils exhibit only weak bioactivities due to the limitation the stability and aqueous solubility. Therefore, in order to give full play to the clinical efficacy of essential oils, new drug formulations need to be developed to promote the healthy and sustainable development of animal husbandry in China.

Tee tree oil (**TTO**) is an essential oil with a fresh camphor odor, light yellow to clear in color (Carson et al., 2006). TTO is extracted from the leaves of the tea tree, native to the coast of southern Queensland to northern New South Wales, Australia (Pazyar et al., 2013). TTO is used to treat acne, herpes, insect bites, scabies, and fungal or bacterial skin infections (Thomas et al., 2016). TTO has a minimum inhibitory concentration of less than 1% against most bacteria and fungi, indicating that TTO has good antibacterial properties (Kong et al.,

Received June 24, 2022.
Accepted October 5, 2022.

[1]Corresponding author: jgli@yzu.edu.cn

2019). The main components of TTO that exert antibacterial effects are terpinen-4-ol and a small amount of α-terpineol, which disrupt the cell membrane of microorganisms and cause cell lysis for bactericidal purposes (Hammer et al., 2012). However, TTO is unstable, insoluble in water, and its active ingredients will change once TTO is exposed to air and oxidized. Therefore, there is an urgent need for developing new dosage forms to improve the clinical application and targeting of TTO.

Nanoliposomes are a bilayer vesicle carrier system that can be formed by self-assembly in aqueous media, which enhances the penetration of its contents into cells through interactions with cells such as adsorption, fusion, and phagocytosis (Moser and Baker, 2021). In recent years, liposomes have made great breakthroughs and are widely used as a drug carrier in various fields such as medicine, food, and cosmetics (Khanniri et al., 2016). This also opens a new path for the development of essential oils in the field of their applied dosage forms. It can overcome the poor stability of essential oils during storage and application.

Colibacillosis is an acute inflammatory response stimulated by bacteria entering the bloodstream and proliferating, eventually colonizing internal organs (Zhu et al., 2017). The main component of the *E. coli* cell wall is lipopolysaccharide (**LPS**), and lysis of the bacteria leads to a massive release of LPS (Li et al., 2018). This process causes an inflammatory response is one of the main pathogenic factors of *E. coli* (Song et al., 2020). NLRP3 is a member of the NOD-like receptor (**NLR**) family, and it is now clear that NLRP3 plays an important role in the inflammatory response induced by *E. coli* (Moody et al., 2014). Stimulation by LPS leads to increased levels of NLRP3 transcripts. Then NLRP3 assembles with proteins involved in the control of apoptosis in the cytoplasm to create the NLRP3 inflammatory vesicle multi-protein complex that identifies and activates Casepase-1, which drives the maturation of IL-1β and IL-18 (Ye et al. 2015). HMGB1 is an important mediator of late-stage inflammation. When cells are under stress, HMGB1 in the nucleus is released into the extracellular compartment and binds to receptors. Then the inflammatory response is amplified by activating the nuclear transcription factor NF-κB, which stimulates the expression and release of pro-inflammatory factors such as TNF-α and IL-1β (Andersson et al., 2018).

Consequently, in order to enhance the stability, aqueous solubility, and efficacy of TTO, this study prepared and optimized tea tree oil nanoliposomes (**TTONL**) and characterized its performance. Furthermore, the in vitro antibacterial activity of TTONL against *E. coli* and the preventive protection against experimental colibacillosis in chickens were investigated.

MATERIALS AND METHODS

Bacterial Strains and Chemical Reagents

The standard strain *E. coli ATCC*25922 is kept in our laboratory. Pigeon-derived *E. coli* clinical isolate named 0419-P_1B_1, was isolated from sick pigeons collected from Jiangsu Wittek Pigeon Co., Ltd. Goose-derived *E. coli* clinical isolate named 0705-E_1H_2, was a generous gift from Dr. Yanhong Wang, school of Veterinary Medicine, Yangzhou University, China. Pig-derived *E. coli* CVCC197 was purchased from China Veterinary Microbial Strain Collection Management Center. The strains were cultured in Luria-Bertani (**LB**) broth under shaking at 37°C to achieve logarithmic growth phases and then were used for further experiments.

Tea tree oil (purity 98%) was purchased from Jiangxi Zhonghuan New Material Co., Ltd., China. Egg Yolk Lecithin (615V021) and Tween-80 (613B052) were both bought from Beijing Solaibio Technology Co., Ltd, China. Cholesterol (EC11BA0007) was obtained from Shanghai Bioengineering Co., Ltd, China. Trichloromethane, n-hexane, methanol, formaldehyde (10010018), and sliced paraffin (69019361) were supplied from Sinopharm Chemical Reagent Co., Ltd., China. Glutathione Peroxidase Assay Kit (S0056), Lipid Oxidation (**MDA**) Assay Kit (S0131S) and Total SOD Activity Assay Kit (S0101S) were purchased from Shanghai Beyotime Biotechnology Co., Ltd., China. Hifair III 1st Strand cDNA Synthesis Kit (11139ES10) and Hifair qPCR SYBR Grenn Master Mix (11201ES03) were obtained from Yeasen Biotechnology (Shanghai) Co., Ltd, China.

Preparation of TTONL

TTONL was prepared by thin film hydration and sonication technique. A certain amount of egg yolk lecithin and cholesterol was weighed into a 50 mL round bottom flask. Ten mL of trichloromethane was added and shaken to form a clear yellow solution, which was placed on a rotary evaporator (RE2000A, Yarong, China) and evaporated at 25 rpm at room temperature to remove the organic solvent.

A certain amount of TTO and Tween-80 was put into a centrifuge tube. After full emulsification, PBS was supplemented until the emulsion system was 10 mL. The TTO emulsion was preheated at 55°C and poured into a round bottom flask with lipid film for rotary hydration. Then the resulting suspension was sonicated for 10 min using an ultrasonic crusher to obtain TTONL (SM650A, Shunma, China).

Box-Behnken Response Surface Method

Based on the single-factor test, 3 factors with significant effects on the encapsulation rate of TTONL were screened: lecithin to cholesterol mass ratio (*X1*), TTO concentration (*X2*), and pH of hydration medium (*X3*), and the encapsulation rate (Y) was used as the response value. Box-behnken method combined with the software Design-Expert 11.0 was used to optimize the design (Table 1).

Characterization

The ultra-micromorphology of the samples was determined by a Tecnai 12 transmission electron microscope (Royal Philips, Netherlands). The particle size,

Table 1. Box-behnken factor level table.

Factor	Code	Level and scope		
		−1	0	1
A Lecithin to cholesterol mass ratio (w/w)	*X1*	3	4	5
B TTO concentration (%)	*X2*	0.2	0.4	0.6
C pH of hydration medium	*X3*	7	7.5	8

polydispersity index (**PDI**), and zeta potential of the samples were determined by a Zetasizer Nano ZS90 nanoparticle size analyzer (Malvern, UK). A Cary 610/670 micro-infrared spectrometer (Agilent Technologies Ltd., Santa Clara, CA) was used to scan in the wave number range of 4,000−500 cm^{-1} to obtain the infrared spectra of each sample.

TTONL was placed at 4°C and room temperature, and samples were taken at 7, 14, 21, 28, and 35 d for the determination of particle size and PDI.

In Vitro Antibacterial Assay

MIC and MBC Referring to the standard published by CLSI, (M100, 2019), the MIC and MBC of TTONL, TTO stock and empty nanoliposomes (ENL) on *E. coli* clinical isolates were determined by micro-broth dilution method in 96-well plates, respectively. Single colonies of the strains to be tested were picked into LB liquid medium and incubated until logarithmic growth phase. Then the number of colonies per well was 1.0×10^6 CFU/mL, and read the results after incubation at 37°C for 16 to 18 h.

***Growth of* E. coli** The standard strain *ATCC*25922 and clinical isolate 0419-P_1B_1 were cultured to logarithmic growth stage. The positive control group, 1MIC group, 1/2MIC group and 1/4MIC group were set up in sterile 96-well plates, incubated at 37°C for 24 h. The OD values of each group at 600 nm were read at 0, 1, 2, 3, 4, 5, 6, 7, 8, 10, 12, and 24 h with an enzyme marker (Bio Tek, Shoreline, WA), and the time growth curves were plotted.

Scanning Electron Microscope Blank control group, 1MIC group, 1/2MIC group, and 1/4MIC group were set up. Except for the control group, the corresponding concentration of TTONL was added to the remaining 3 groups. Then, 100 μL of clinical isolate 0419-P_1B_1, which was pre-cultured to logarithmic growth stage, was incubated for 4 h at 37°C. The groups of bacterial precipitates were obtained by centrifugation at 4,000 rpm for 10 min, and added 1 mL glutaraldehyde fixative to resuspend and store overnight at 4°C.

The prepared samples were observed and photographed on the SEM after cleaning, dehydration, drying, gluing and gold spraying (GeminiSEM 300, Carl Zeiss AG).

In Vivo Experiment

Animals The one-day-old yellow-feathered broiler chickens (male) were purchased from Jiangsu Poultry Research Institute and housed in the animal house of the College of Veterinary Medicine, Yangzhou University, China. The rearing environment and cages were disinfected by formaldehyde and potassium permanganate fumigation to ensure a uniform test environment with no other influencing factors. The cages were kept at uniform density, lit by 40 W light bulbs and maintained the temperature of the breeding environment by electric heaters. The full price chicken feed was provided by Jiangsu Provincial Poultry Research Institute, China, and it was chicken feed without any drugs and additives.

Experiments Designs

One hundred and twenty, 1-day-old healthy chickens were selected and kept normally for 14 d, then randomly divided into 6 groups. The 6 groups were named blank control group, *E. coli* 0419P_1B_1 group, *E. coli* 0419P_1B_1+TTONL (5 mg/kg, 10 mg/kg, 20 mg/kg) group and DOX group. The different concentrations of TTONL and DOX were intragastrically administered once daily for 3 d before *E. coli* 0419P_1B_1 infection. Then single colonies of *E. coli* 0419P_1B_1 were picked from the medium, incubated for 12 h and centrifuged at 4,000 rpm for 10 min. Concentration of bacterial solution was adjusted to 4×10^9 CFU/mL. The blank control group was injected with 0.5-mL saline intramuscularly once per chicken, and the remaining groups were injected with 0.5 mL bacterial solution intramuscularly once per chicken. Samples were collected 12 h after infection for the detection of relevant indexes.

Liver Bacterial Load

The liver tissues of chickens in each group were collected aseptically, placed in 4-mL centrifuge tubes. The same number of grinding beads and a certain amount of sterile PBS were added to grind with homogenizer. A total of 100 μL of liver homogenate was took on LB solid medium, and incubated at 37°C for 24 h for observation and counting.

Histopathology in Duodenal and Cecum

Duodenum and cecum tissues were washed with PBS and then fixed in 4% paraformaldehyde for 24 h. The fixed tissues were made into paraffin block after a series of procedure, such as dehydration with gradient ethanol, clarity with xylene, waxdip, and so on. Then the paraffin block was sliced into 4 μm sections. Ultimately, the sections were stained with hematoxylin and eosin (**HE**) and examined by microscopy for the histopathological changes.

Duodenal Villus Height, Crypt Depth, and Ratio V/C

Using imageJ image analysis software, the pixel values of villi height and crypt depth (n = 5) were measured for each group of duodenal HE images at 20× field of view.

Table 2. Primer sequences for qRT-PCR.

Gene	Forward primer	Reverse primer
NLRP3	CGGCATCTGGAAGCACAAGG	GAAACTGCCCAACACGCTCT
NF-κB(p65)	CAGCCCATCTATGACAACCG	TCAGCCCAGAAACGAACCTC
GAPDH	GAGAAACCAGCCAAGTATGATGA	CTTGACGAAATGGTCATTCAGT

The data were converted at 1.12 μm/pixel, and the ratio of villi height to crypt depth (V/C) was calculated.

Real-Time Fluorescent Quantitative PCR

Total RNA was extracted from duodenum and cecum tissue samples using Trizol reagent following the manufactures' instructions. Its concentrations and quality were determined by the nanodrop spectrophotometer (Thermo Scientific, Wilmington, DE), and cDNA synthesized using Hiscript II QRT supermax. Real-time quantitative PCR (**RT-qPCR**) was performed with the cfx96 real-time system (Bio-Rad, Hercules, CA). Templates without cDNA were used as negative controls for each gene in each test. The relative quantitative results were calculated by the $2^{-\Delta\Delta Ct}$ method, $\Delta Ct = CT\text{-}CT_{actin}$, $-\Delta\Delta Ct = -(\Delta Ct_{experimental\ group} - \Delta Ct_{blank\ group})$. The primer sequences NLRP3 and NF-κB(p65) were designed (Table 2). Data are representative of three independent experiments.

Statistical Analysis

The experimental data were analyzed using SSPS 25.0 statistic software and at least 3 independent replicates. Statistical analysis was determined using a one-way analysis of variance (**ANOVA**) with Duncan the multiple-comparison test. The results were expressed as mean ± SE and represented with GraphPad Prism 8.0 to make the histogram and curves. $P < 0.05$ was considered as significant difference and $P < 0.01$ was extremely significant difference.

RESULTS

Optimization of Response Surface Method

A quadratic regression orthogonal combination test with 3 factors and 3 levels of 17 test points was designed using the BBD response surface method, with the encapsulation rate as the response value. After the quadratic regression fitting, the fitted equation of the relationship between the sealing rate Y and the influencing factor X was obtained:

$$Y = +79.74 + 0.1663X_1 + 7.27X_2 - 2.04X_3 - 0.5700X_1 + 5.57X_1X_3 - 0.2725X_2X_3 - 2.47X_1^2 - 8.76X_2^2 - 7.16X_3^2$$

It can be seen that the model is highly significant (P model < 0.0001), with a non-significant $P = 0.0589$ for the misfit term. Correlation $R^2 = 0.9821$, correction coefficient of determination $R_{Adj^2} = 0.9591$, with a difference of less than 0.2 from the prediction coefficient of determination $R_{Pred^2} = 0.7612$. From these results, it can be concluded that this model fits well (Table 3).

The optimal values of TTONL encapsulation rate occur at a hydration medium pH between 7.2 and 7.4 and the lecithin to cholesterol mass ratio between 3.5 and 4. The optimal value of TTONL encapsulation rate occurs at lecithin to cholesterol mass ratio between 3.5-4.5 and TTO concentration between 0.4-0.6. The optimum value of TTONL encapsulation rate occurs at a TTO concentration between 0.4 and 0.6 and a hydration medium pH between 7.2 and 7.6 (Figure 1).

Table 3. Response surface model ANOVA.

Source	Sum of squares	df	Mean square	F value	Prob>F
Model	1198.31	9	133.15	42.73	< 0.0001 Significant
A	0.2211	1	0.2211	0.0710	0.7976
B	422.97	1	422.97	135.74	< 0.0001
C	33.21	1	33.21	10.66	0.0138
AB	1.30	1	1.30	0.4171	0.5390
AC	123.99	1	123.99	39.79	0.0004
BC	0.2970	1	0.2970	0.0953	0.7665
A^2	25.71	1	25.71	8.25	0.0239
B^2	323.18	1	323.18	103.72	< 0.0001
C^2	216.07	1	216.07	69.34	< 0.0001
Residual	21.81	7	3.12		
Lack of fit	17.82	3	5.94	5.95	0.0589 Not significant
Pure error	3.99	4	0.9985		
Cor total	1220.13	16			

$R^2 = 0.9821$, $R_{Adj}{}^2 = 0.9591$, $R_{Pred}{}^2 = 0.7612$.

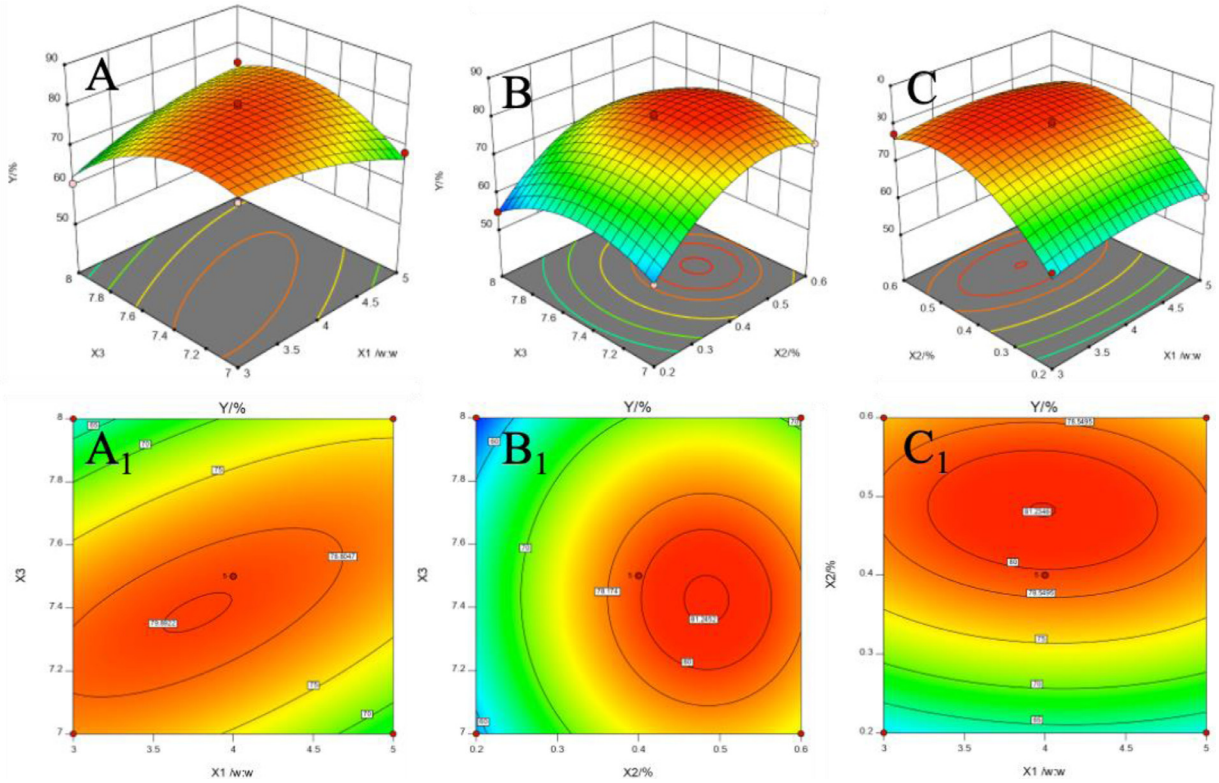

Figure 1. Response surface and contour map. (A-A_1) Lecithin to cholesterol mass ratio vs. hydration medium pH, (B-B_1) Lecithin to cholesterol mass ratio vs. TTO concentration, (C-C_1) TTO concentration vs. hydration medium pH. Abbreviation: TTO, tee tree oil.

After optimization of the TTONL preparation conditions by single-factor and response surface tests, the optimal preparation conditions were obtained: lecithin to cholesterol mass ratio of 3.7:1, TTO concentration of 0.5, and pH of the hydration medium of 7.4.

Characterization of TTONL

Transmission electron microscope (**TEM**) analysis showed that ENL presented as a ring fingerprint multilayer microcapsule structure, with a clearly visible bilayer structure and a single chamber inside. TTONL had a thickened membrane structure and a dark shadow inside, indicating that TTO was encapsulated into the aqueous compartment of the liposome (Figure 2A). The average particle size of TTONL was 227.8 ± 25.3 nm, PDI was 0.165 ± 0.05, the average particle size of ENL was 491.1 ± 51.7 nm, PDI was 0.312 ± 0.07 (Figure 2B). The particle size of TTONL was smaller and more uniformly dispersed than that of ENL, the zeta potential of ENL was about −14.8 mV, while that of TTONL was reduced to −2.08 mV. The zeta potential of ENL was about −14.8 mV, while that of TTONL was reduced to −2.08 mV (Figure 2C). The characteristic peak of the ether bond of TTO showed at 1300 to 1,000 cm^{-1}, and the characteristic absorption peak here disappears in TTONL, indicating that TTO was encapsulated into the inner cavity of ENL. The characteristic absorption peaks of ENL and TTONL seemed not change much, indicating that the basic skeleton of liposome did not change greatly (Figure 2D).

Comparison of Stability Between TTONL and TTO During Storage

The particle size and PDI of TTONL under different storage conditions increased slowly over 35 d. The particle size of TTONL at 4°C increased from 199.1 ± 1.74 nm to 224.20 ± 2.54 nm, with a change of 12.6%. The particle size of TTONL at room temperature increased from 199.1 ± 1.74 nm to 276.45 ± 2.61 nm, with a change of 38.8% (Figure 3A). The PDI of TTONL increased from 0.133 to 0.178 and 0.185 at 4°C and room temperature, with a change of 33.8 and 39.1%, respectively (Figure 3B). The results indicated that TTONL at 4°C was more stable than at room temperature.

TTONL Inhibited E. coli in Vitro

TTONL showed good inhibition and bactericidal effects on the tested strains (Table 4), with MIC of 0.75 mg/mL and MBC of 1.50 mg/mL. The MIC and MBC of TTONL were 4-fold lower than TTO stock solution, and blank liposomes had no significant inhibitory effect on the tested strains.

TTONL showed significant bactericidal effect on both the standard strain *ATCC*25922 (Figure 4A) and clinical isolate 0419-P_1B_1 (Figure 4B). The bactericidal activity of TTONL was positively correlated with the concentration, with 0.38 mg/mL and 0.19 mg/mL of TTONL had an inhibitory effect on the growth of the strains. While the treatment with

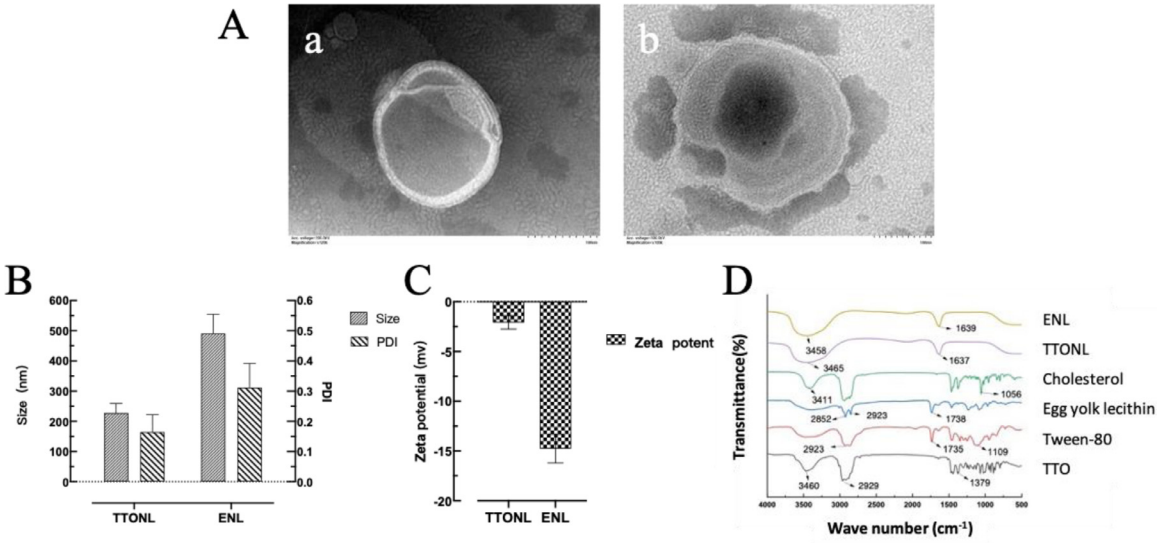

Figure 2. Characterization of TTONL. (A) TEM of ENL (a) and TTONL (b) (100 kV). (B) Mean particle size of ENL and TTONL (n = 3). (C) Mean zeta potential of ENL and TTONL (n = 3). (D) FTIR spectra of TTO, ENL, TTONL, cholesterol, egg yolk lecithin, and Tween-80. Abbreviations: ENL, empty nanoliposomes; TEM, transmission electron microscope; TTO, tee tree oil, TTONL, tee tree oil nanoliposomes.

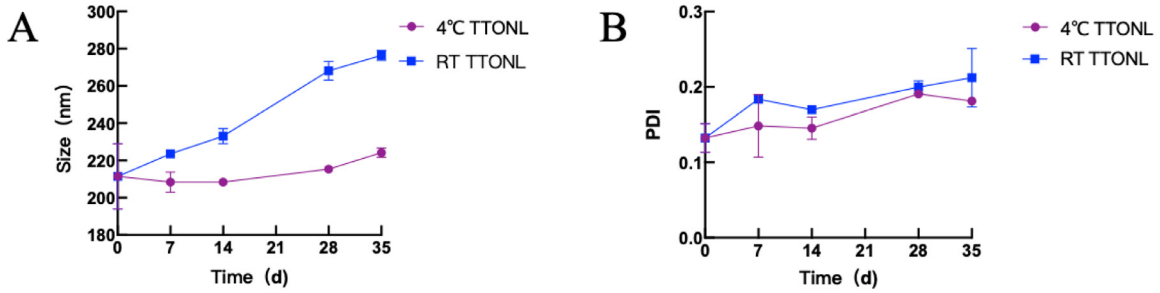

Figure 3. The stability of TTONL at 4°C and room temperature. (A) Particle size change of TTONL over 35 days (n = 3). (B) PDI change of TTONL over 35 days (n = 3). Abbreviations: TTONL, tee tree oil nanoliposomes.

0.75 mg/mL of TTONL had fully achieved the bactericidal effect at 8 h.

SEM analysis of the blank control, 1MIC, 1/2MIC, and 1/4MIC groups showed that normal *E. coli* had a short rod-like morphology (Figure 4C). *E. coli* treated with TTONL showed different degrees of damage and changes in surface morphology. The membrane surface of *E. coli* treated with 0.75 mg/mL (1MIC) TTONL exhibited swelling, distortion, and individual deformation (Figure 4C-b). *E. coli* treated with 0.38 mg/mL (1/2MIC) TTONL showed significant elongation (Figure 4C-c). The membrane surface of *E. coli* treated with 0.19 mg/mL (1/4MIC) TTONL was also slightly damaged (Figure 4C-d).

Effects of TTONL on Body Weight and Liver Bacterial Load in Broilers Challenged by E. coli

After *E. coli* infection, body weight gain in the model group was slowed down significantly. While growth restriction was alleviated in all TTONL groups, and the effect was better than that of the Dox group (Figure 5A). The *E. coli* load in liver tissues was detected by smear plate counting (Figure 5B). The bacterial load in liver tissues was significantly increased after *E. coli* 0419-P_1B_1 infection, and pretreatment with different concentrations of TTONL was able to significantly reduce the load of *E. coli* 0419-P_1B_1 in liver tissues. The effect of TTONL on bacterial load in liver had a dose-dependent, with the high concentration TTONL group (20 mg/kg) achieved the effect of Dox positive control group. These results suggested that TTONL could improve the growth and decrease the bacterial load in liver tissues of *E. coli* infected chickens to a certain extent.

TTONL Alleviated the Intestinal Damage of Broilers Challenged by E. coli

The intestinal villi of the cecum were shortened and crumpled after *E. coli* challenged, while the damage to the intestinal villi in the TTONL pretreatment groups were less severe compared with the model group. The intestinal villi in the TTONL high dose (20 mg/kg) group was more intact without shedding and inflammatory cell

Table 4. MIC/MBC assay results of TTO, TTONL, and ENL on 4 tested *E. coli* strains.

Medicine (mg/mL)	Antibacterial activity	Test strains			
		*ATCC*25922	CVCC197	0419-P_1B_1	0705-E_1H_2
TTO	MIC	3.00	3.00	3.00	3.00
	MBC	6.00	6.00	6.00	6.00
TTONL	MIC	0.75	0.75	0.75	0.75
	MBC	1.50	1.50	1.50	1.50
ENL	MIC	–	–	–	–
	MBC	–	–	–	–

Abbreviations: ENL, empty nanoliposomes, TTO, tee tree oil, TTONL, tee tree oil nanoliposomes.

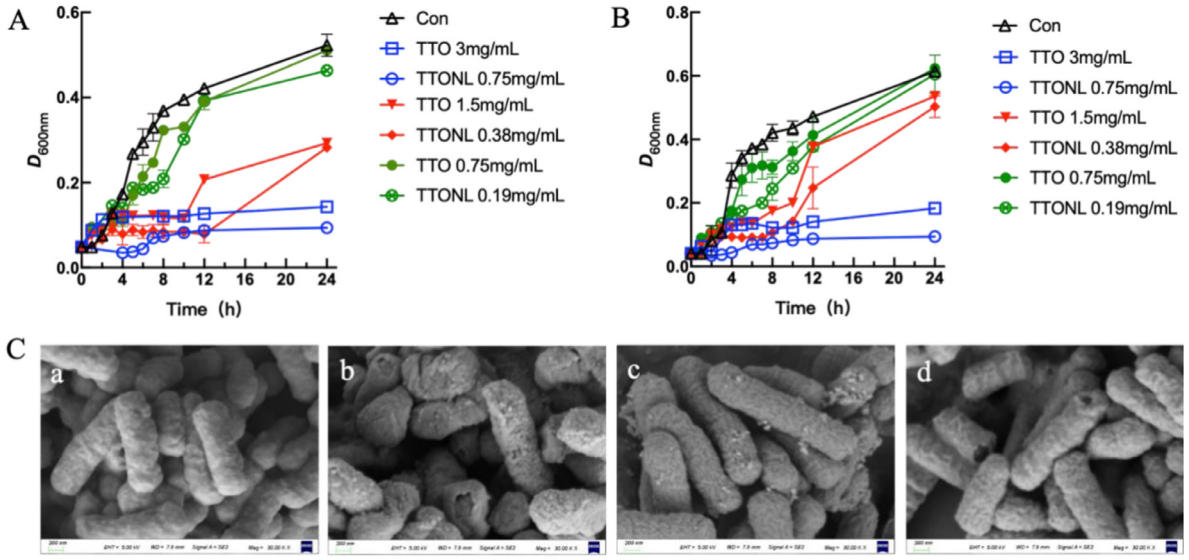

Figure 4. Inhibition of growth and damage of *E. coli* by TTONL. (A) Effect of TTO and TTONL on the growth of *ATCC*25922. (B) Effect of TTO and TTONL on the growth of 0419-P_1B_1. (C) SEM results of *E. coli* treated with different concentrations of TTONL (30KX). (a) Control, (b) 1MIC (0.75 mg/mL), (c) 1/2MIC (0.38 mg/mL), (d) 1/4MIC (0.19 mg/mL). Abbreviations: TTO, tee tree oil, TTONL, tee tree oil nanoliposomes.

infiltration (Figure 6A). The pathological damage of the duodenum in each group was mainly reflected in the morphological changes of the crypt. Distortion and atrophy of the crypt were observed in the model group, while the degree of crypt damage was less in the TTONL pretreated groups compared to the model group (Figure 6B). These results suggested that TTONL significantly reduced the extent of damage to chicken intestinal tissues by *E. coli* infection. The chorionic villus height in the model group was lower than that in the blank group, and the chorionic villus height in the medium and high dose TTONL groups (10 and 20 mg/kg) and the Dox group was higher than that in the model group (Figure 6C). The crypt depth in the model group was significantly higher than that in the blank group, and the crypt depth in both the TTONL and Dox groups was significantly lower compared to that in the model group (Figure 6D). The chorionic villus ratio in the model group was significantly smaller than that in the blank group, and the TTONL and Dox groups were significantly higher than that in the blank group (Figure 6E).

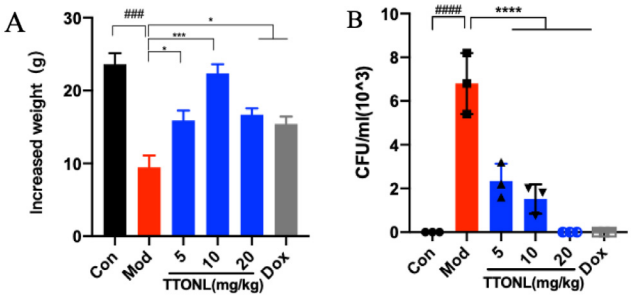

Figure 5. TTONL relieved weight loss and elevated bacterial load of broilers. (A) The increased weight of broilers. (B) The bacterial load in liver tissues. The data are expressed as the Mean ± SE (n = 20). * $P < 0.05$ vs. mod, ** $P < 0.01$ vs. mod, *** $P < 0.001$ vs. mod, **** $P < 0.0001$ vs. mod, ### $P < 0.001$ vs. con, #### $P < 0.0001$ vs. con. Abbreviation: TTONL, tee tree oil nanoliposomes.

TTONL Reduced the Expression Level of NLRP3 and NF-KB (p65) Genes Induced by E. coli *in the Broilers Intestine*

The mRNA expression of NLRP3 and NF-κB (p65) were significantly elevated in the duodenum and cecum of chickens in the model group (Figure 7). The mRNA expression of NLRP3 was significantly decreased in the TTONL prevention groups at all concentrations. The mRNA expression of NF-κB (p65) was significantly

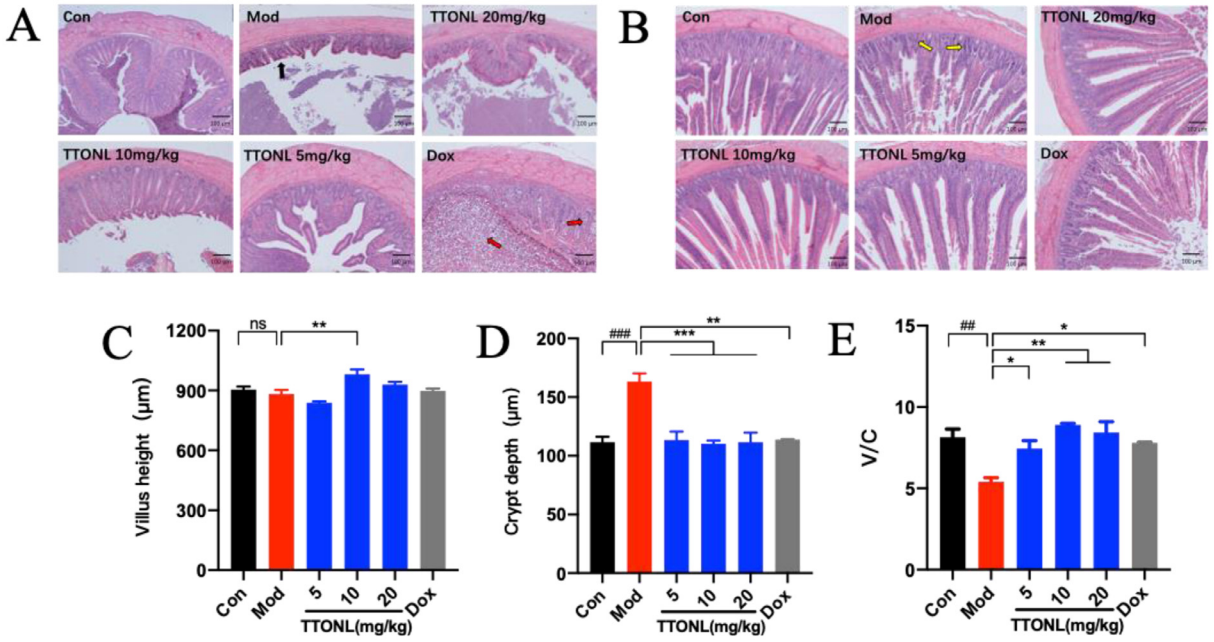

Figure 6. TTONL relieved the intestinal damage caused by *E. coli* 0419-P_1B_1 in broilers. (A) Histological changes in the cecum (100X). (B) Histological changes in the duodenum (100X). (C) The duodenal villus height. (D) The duodenal crypt depth. (E) The duodenal villus height / crypt depth. The data are expressed as the Mean ± SE (n = 6). * $P < 0.05$ vs. mod, ** $P < 0.01$ vs. mod, *** $P < 0.001$ vs. mod, ## $P < 0.01$ vs. con, ### $P < 0.001$ vs. con, ns means no significant vs. con/mod. Abbreviation: TTONL, tee tree oil nanoliposomes.

decreased in the TTONL high-dose group compared with the model group.

DISCUSSION

In order to optimize the drug manufacture process and prescription screening, domestic scholars have frequently employed uniform design and orthogonal design. These 2 approaches are distinguished by a small number of tests, straightforward experimental data processing, and straightforward operation (He et al., 2019). However, as both methods are dependent on linear mathematical models, the testing precision is inadequate. The chosen test value is only near to the ideal value, and the optimal point cannot be precisely determined (Hamzah et al., 2015). In addition, the conceivable interactions between diverse parameters have not been exhaustively investigated, resulting in a low experimental precision (Zheng et al., 2020). Box-behnken response surface approach is a multifactor nonlinear test optimization method. This technology is more appropriate for multifactor 3-level tests than the orthogonal design method, due to its fewer tests, higher test accuracy, and simpler and more exhaustive (Chua et al., 2020). This method's fitted equation can predict the value of any test point within the test range with great accuracy, hence presenting a distinct advantage (Chan et al., 2019). Therefore, a three level-three variable BBD was adopted in this study, and 17 experiments were required to establish optimum conditions for the preparation of TTONL.

The particle size of TTONL decreased by 270 nm compared to blank liposomes suggested that the addition of essential oils could reduce the particle size of liposomes. Because the insertion of essential oils into the surface of liposome membranes increases fluidity and decreases membrane strength (Ruozi et al., 2007). In addition, essential oils can produce stronger polymerization forces between the nonpolar chains of membrane vesicles, hence increasing the surface curvature of yolk lecithin vesicles when ultrasonic energy is applied (Valenti et al., 2001).

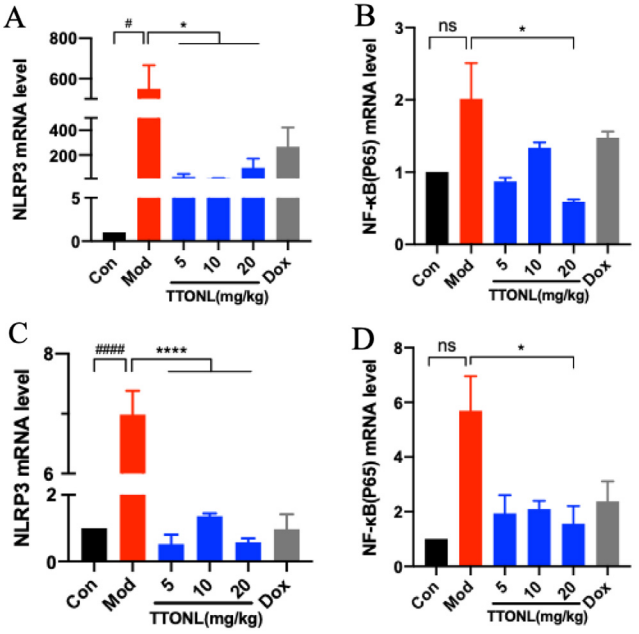

Figure 7. Relative expression of inflammatory genes in broilers. (A) NLRP3 in duodenum. (B) NF-κB(p65) in duodenum. (C) NLRP3 in cecum. (D) NF-κB(p65) in cecum. The data are expressed as the Mean ± SE (n = 4). * $P < 0.05$ vs. mod, **** $P < 0.0001$ vs. mod, # $P < 0.05$ vs. con, #### $P < 0.0001$ vs. con, ns means no significant vs. con/mod.

Within 35 d, the particle size of TTONL changed by just 25 nm, representing a change of approximately 12%, and the PDI value increased by only 0.045. The changes of particle size and PDI served as indications for determining whether or not the liposomes were agglomerated. Tween-80, as a nonionic surfactant, generated a spatial site resistance effect on the surface of the liposomes and formed a highly stable liposome dispersion system (Dhingra et al., 2013), which may account for the relatively good stability of TTONL. Fourier transform infrared spectroscopy (**FTIR**) is the measurement of the interaction of infrared radiation with substances by absorption, emission or reflection. About 1,300−1,000 cm^{-1} is the characteristic peak of the ether bond in the molecular structure of TTO. The characteristic peak here disappeared when TTONL was detected, indicating that TTO was encapsulated into the liposome. While the characteristic absorption peak of the liposome changes from 1,639 cm^{-1} and 3,458 cm^{-1} to 1,637 cm^{-1} and 3,465 cm^{-1} due to the stretching vibration of the chemical bond (Tiernan et al., 2020).

Similar to protoplasts, liposomes have a lipid bilayer structure (Bertrand et al., 2010). Liposomes with a lecithin component interact with cells (contact release, intermembrane transfer, fusion, phagocytosis, uptake, etc.), increasing the permeability of essential oils to cells (Torchilin, 1996). Compared to TTO prodrug, this interaction of TTONL with cells results in TTO selectively ignoring molecular recognition of outer membranes, thus providing better inhibition of bacteria with lipid membrane structures. Liposomes' membrane structure is comparable to that of biological cell membranes. As a result, it is histocompatible as a medication carrier (Mozafari et al., 2008; Tada et al., 2018). Previous research found that encapsulating essential oils in liposomes significantly increased their antibacterial activity (Longbottom et al., 2004; Kang et al. 2018). This was consistent with the results of the drug sensitivity tests in this study. The MIC and MBC of TTONL for *E. coli* were about 4-fold lower than those of TTO, indicating that the inhibitory effect of TTONL on *E. coli* was stronger than that of TTO. Additionally, the essential oil is encapsulated inside the liposomes and has a slow-release property, which enables TTONL to overcome the weakness of volatile essential oils and provide a long-lasting bactericidal effect. The integrity of the cell membrane is critical to the survival of bacteria, also is a key factor in maintaining basal intracellular metabolism. Disruption of the integrity of the cell membrane then leads to bacterial death (Djihane et al., 2017). *E. coli* treated with TTONL showed aberrated morphology and breakage on the cell membrane surface. These results suggested that TTONL had an irreversible destructive damage effect on *E. coli* cells, leading to the breakage of bacterial cell membranes and leakage of intracellular contents. This is consistent with previous study reporting that active ingredients of TTO damage the bacterial cell membrane (Kim et al., 2014). This result also indicated that the bacterial cell membrane was the primary target of essential oils.

E. coli is a Gram-negative, pathogenic, anaerobic, rod-shaped bacterium that is usually found in the lower gastrointestinal tract of thermostatic animals (Koonin et al., 2017). TTONL pretreatment was able to improve the body weight and reduce liver bacterial load of chicken caused by *E. coli*. In addition, it could also significantly increase the height of intestinal villi in chickens. Probably the active substances in TTO release from liposomes, such as pineolene and α-pinene, promote the development of villi and thus improve the integrity of the intestinal mucosa, reduce the invasion and colonization of the intestine by *E. coli*.

TTONL pretreatment significantly inhibited pathological injury and expression of inflammatory cytokines NLRP3, NF-κB (p65) in the duodenum and cecum. NLRP3 plays an important role in microbial-induced inflammatory responses, forming inflammatory vesicles that recognize and activate Casepase-1 in the presence of activated followed by the induction of IL-1β and IL-18 maturation (Pétrilli et al., 2007; Kelley et al., 2019; Ju et al., 2021). Oral administration of TTONL effectively alleviated intestinal inflammation and significantly downregulated the expression of NLRP3. Terpinen-4-ol, the main component of TTO, has been reported to effectively inhibit the expression of inflammatory cytokines produced as a result of LPS stimulation, thus playing a major regulatory role in the anti-inflammatory process (Nogueira et al., 2014). It is thus hypothesized that TTONL also exerts its anti-inflammatory effects through the active ingredient terpinen-4-ol. The activation of NLRP3 cannot be separated from NF-κB-mediated signaling activation, which is initiated by upregulating the transcription of inflammatory vesicle-related components, such as NLRP3, IL-18 precursor (pro-IL-18), and IL-1β precursor (pro-IL-1β) (Ju et al., 2021). In addition, NF-κB is able to specifically bind to κB sites on different gene promoters to promote transcriptional regulation of target genes, among which the p65 site has significant pro-inflammatory properties. Thus NF-κB (p65) plays a key role in inflammation and immune response, among others (Li et al., 2015). The significant downregulation of NF-κB (p65) treated by TTONL, indicating that TTONL plays a key role in inflammation by inhibiting NF-κB (p65) activity.

CONCLUSIONS

Our results confirmed that TTONL produced by response surface methodology had higher encapsulation rate, better stability, and slow release. In addition, TTONL showed good inhibitory and inactivating effects on all 3 *E. coli* clinical isolates. Prophylactic administration of TTONL alleviated *E. coli*-induced organismal damage, significantly downregulated mRNA expression of NLRP3 and NF-κB (P65) in the duodenum and cecum of chickens infected by *E. coli*. These findings provided a novel insight into the potential prophylactic application of TTONL to avian bacterial diseases.

ACKNOWLEDGMENTS

This work was supported through research projects from the National Science Foundation of China (Grant No. 32072911, 32002324), Natural Science Foundation of Jiangsu Province (Grant No. BK2020945) and the Priority Academic Program Development of Jiangsu Higher Education Institutions (PAPD). We are grateful to all of the other staff members at the Institute of Traditional Chinese Veterinary Medicine of Yangzhou University for their assistance in this study.

Ethical standards: The animal experiment was conducted with an approval from and under the supervision of the Laboratory Animal Welfare Ethics Committee of the Yangzhou University.

DISCLOSURES

All authors of this paper declare no conflict of interest.

REFERENCES

Andersson, U., H. Yang, and H. Harris. 2018. Extracellular HMGB1 as a therapeutic target in inflammatory diseases? Expert Opin. Ther. Targets. 22:263–277.

Bertrand, N., C. Bouvet, P. Moreau, and J. C. Leroux. 2010. Transmembrane pH-gradient liposomes to treat cardiovascular drug intoxication. ACS Nano 4:7552–7558.

Carson, C. F., K. A. Hammer, and T. V. Riley. 2006. Melaleuca alternifolia (Tea Tree) oil: a review of antimicrobial and other medicinal properties. Clin. Microbiol. Rev. 19:50–62.

Chan, Y. T., M. C. Tan, and N. L. Chin. 2019. Application of Box-Behnken design in optimization of ultrasound effect on apple pectin as sugar replacer. LWT 115:108449.

Chua, S. C., F. K. Chong, C. H. Yen, and Y. C. Ho. 2020. Evaluation and optimization of the coagulation-flocculation process using conventional rice starch in potable water treatment. IOP Conf. Series: Mater. Sci. Eng. 736:072009.

Dhingra, S., M. Morita, T. Yoda, M. C. Vestergaard, T. Hamada, and M. Takagi. 2013. Dynamic morphological changes induced by GM1 and protein interactions on the surface of cell-sized liposomes. Mater 6:2522–2533.

Djihane, B., N. Wafa, S. Elkhamssa, D. H. J. Pedro, A. E. Maria, and Z. M. Mihoub. 2017. Chemical constituents of Helichrysum italicum (Roth) G. Don essential oil and their antimicrobial activity against Gram-positive and Gram-negative bacteria, filamentous fungi and Candida albicans. Saudi Pharm. J. 25:780–787.

Hammer, K. A., C. F. Carson, and T. V. Riley. 2012. Effects of Melaleuca alternifolia (tea tree) essential oil and the major monoterpene component terpinen-4-ol on the development of single- and multistep antibiotic resistance and antimicrobial susceptibility. Antimicrob. Agents Chemother. 56:909–915.

Hamzah, M. O., S. R. Omranian, B. Golchin, and M. R. Hainin. 2015. Evaluation of effects of extended short-term aging on the rheological properties of asphalt binders at intermediate temperatures using respond surface method. J. Teknol. 73:133–139.

He, H. S., Y. Lu, J. P. Qi, Q. G. Zhu, Z. J. Chen, and W. Wu. 2019. Adapting liposomes for oral drug delivery. Acta Pharm. Sin. B. 9:46–58.

Holmes, A. H., L. S. P. Moore, A. Sundsfjord, M. Steinbakk, S. Regmi, A. Karkey, P. J. Guerin, and L. J. V. Piddock. 2016. Understanding the mechanisms and drivers of antimicrobial resistance. Lancet 387:176–187.

Ju, M. Y., J. Bi, Q. Wei, L. Y. Jiang, Q. T. Guan, M. Zhang, X. Y. Song, T. Chen, J. Y. Fan, X. J. Li, M. J. Wei, and L. Zhao. 2021. Pan-cancer analysis of NLRP3 inflammasome with potential implications in prognosis and immunotherapy in human cancer. Brief. Bioinform. 22:1–16.

Kang, C. Y., Q. K. Wang, and J. B. Wang. 2018. Comparison of the inhibition effect of cinnamaldehyde liposomes on three species of pathogenic bacteria in aquatic animals. Jiangsu. Ag. Sci. 46:176–178.

Kelley, N., D. Jeltema, Y. H. Duan, and Y. He. 2019. The NLRP3 inflammasome: an overview of mechanisms of activation and regulation. Int. J. Mol. Sci. 20:3328.

Khanniri, E., N. Bagheripoor-Fallah, S. Sohrabvandi, A. M. Mortazavian, K. Khosravi-Darani, and R. Mohammad. 2016. Application of liposomes in some dairy products. Crit. Rev. Food Sci. Nutr. 56:484–493.

Kim, S., M. S. Lee, B. Lee, W. G. Gwon, E. J. Joung, N. Y. Yoon, and H. R. Kim. 2014. Anti-inflammatory effects of sargachromenol-rich ethanolic extract of Myagropsis myagroides on lipopolysaccharide-stimulated BV-2 cells. BMC Complement Altern. Med. 14:231.

Kong, C. H., T. D. Xuan, T. D. Khanh, H. D. Tran, and N. T. Trung. 2019. Allelochemicals and signaling chemicals in plants. Molecules. 24:2737.

Koonin, E. V., K. S. Makarova, and Y. I. Wolf. 2017. Evolutionary genomics of defense systems in archaea and bacteria. Annu. Rev. Microbiol. 71:233–261.

Li, G. F., J. H. Fu, Y. Zhao, K. Q. Ji, T. Luan, and B. Zang. 2015. Alpha-lipoic acid exerts anti-inflammatory effects on lipopolysaccharide-stimulated rat mesangial cells via inhibition of nuclear factor kappa B (NF-κB) signaling pathway. Inflammation 38:510–519.

Li, R. X., J. Li, S. Y. Zhang, Y. L. Mi, and C. Q. Zhang. 2018. Attenuating effect of melatonin on lipopolysaccharide-induced chicken small intestine inflammation. Poult. Sci. 97:2295–2302.

Lim, J. Y., J. Yoon, and C. J. Hovde. 2010. A brief overview of Escherichia coli O157:H7 and its plasmid O157. J. Microbiol. Biotechnol. 20:5–14.

Longbottom, C. J., C. F. Carson, K. A. Hammer, B. J. Mee, and T. V. Riley. 2004. Tolerance of Pseudomonas aeruginosa to Melaleuca alternifolia (tea tree) oil is associated with the outer membrane and energy-dependent cellular processes. J. Antimicrob. Chemother. 54:386–392.

Moody, M. A., S. Santra, N. A. Vandergrift, L. L. Sutherland, T. C. Gurley, M. S. Drinker, A. A. Allen, S. M. Xia, R. R. Meyerhoff, R. Parks, K. E. Lloyd, D. Easterhoff, S. M. Alam, H. X. Liao, B. M. Ward, G. Ferrari, D. C. Montefiori, G. D. Tomaras, R. A. Seder, N. L. Letvin, and B. F. Haynes. 2014. Toll-like receptor 7/8 (TLR7/8) and TLR9 agonists cooperate to enhance HIV-1 envelope antibody responses in rhesus macaques. J. Virol. 88:3329–3339.

Moser, M. R., and C. A. Baker. 2021. Taylor dispersion analysis in fused silica capillaries: a tutorial review. Anal. Methods. 13:2357–2373.

Mozafari, M. R., C. Johnson, S. Hatziantoniou, and C. Demetzos. 2008. Nanoliposomes and their applications in food nanotechnology. J. Liposome Res. 18:309–327.

Nogueira, M. N. M., S. G. Aquino, C. R. Junior, and D. M. P. Spolidorio. 2014. Terpinen-4-ol and alpha-terpineol (tea tree oil components) inhibit the production of IL-1β, IL-6 and IL-10 on human macrophages. Inflamm. Res. 63:769–778.

Pazyar, N., R. Yaghoobi, N. Bagherani, and A. Kazerouni. 2013. A review of applications of tea tree oil in dermatology. Int. J. Dermatol. 52:784–790.

Pétrilli, V., S. Papin, C. Dostert, A. Mayor, F. Martinon, and J. Tschopp. 2007. Activation of the NALP3 inflammasome is triggered by low intracellular potassium concentration. Cell Death Differ 14:1583–1589.

Ruozi, B., G. Tosi, E. Leo, and M. A. Vandelli. 2007. Application of atomic force microscopy to characterize liposomes as drug and gene carriers. Talanta 73:12–22.

Song, X. J., H. Y. Jiang, Z. Qi, X. Shen, M. Xue, J. A. Hu, H. M. Liu, X. H. Zhou, J. Tu, and K. Z. Qi. 2020. APEC infection affects cytokine-cytokine receptor interaction and cell cycle pathways in chicken trachea. Res. Vet. Sci. 130:144–152.

Tada, R., H. Suzuki, S. Takahashi, Y. Negishi, H. Kiyono, J. Kunisawa, and Y. Aramaki. 2018. Nasal vaccination with pneumococcal surface protein A in combination with cationic liposomes consisting of DOTAP and DC-chol confers antigen-mediated protective immunity against Streptococcus pneumoniae infections in mice. Int. Immunopharmacol. 61:385–393.

Thomas, J., C. F. Carson, G. M. Peterson, S. F. Walton, K. A. Hammer, M. Naunton, R. C. Davey, T. Spelman, P. Dettwiller, G. Kyle, G. M. Cooper, and K. E. Baby. 2016. Therapeutic potential of tea tree oil for scabies. Am. J. Trop. Med. Hyg. 94:258–266.

Tiernan, H., B. Byrne, and S. G. Kazarian. 2020. ATR-FTIR spectroscopy and spectroscopic imaging for the analysis of biopharmaceuticals. Spectrochim. Acta. A. 241:118636.

Torchilin, V. P. 1996. Liposomes as delivery agents for medical imaging. Mol. Med. Today. 2:242–249.

Valenti, D., A. D. Logu, G. Loy, C. Sinico, L. Bonsignore, F. Cottiglia, D. Garau, and A. M. Fadda. 2001. Liposome-incorporated santolina insularis essential oil: preparation, characterization and in vitro antiviral activity. J. Liposome Res. 11:73–90.

Yang, S. K., N. P. Tan, C. W. Chong, A. Abushelaibi, S. H. E. Lim, and K. S. Lai. 2021. The missing piece: recent approaches investigating the antimicrobial mode of action of essential oils. Evol. Bioinform. 17:1–6.

Ye, J. H., M. Yu, K. Z. Zhang, J. X. Liu, Q. N. Wang, P. Tao, K. Jia, M. Liao, and Z. Y. Ning. 2015. Tissue-specific expression pattern and histological distribution of NLRP3 in Chinese yellow chicken. Vet. Res. Commun. 39:171–177.

Zhao, Y. L., H. T. Li, S. Z. Wei, X. L. Zhou, and X. H. Xiao. 2019. Antimicrobial effects of chemical compounds isolated from traditional Chinese Herbal Medicine (TCHM) against drug-resistant vacteria: a review paper. Mini. Rev. Med. Chem. 19:125–137.

Zheng, Y. Z., T. D. Manh, N. D.Nam, M. B. Gerdroodbary, R. Moradi, and I. Tlili. 2020. Optimization of micro Knudsen gas sensor for high precision detection of SO2 in natural gas. Results Phys 16:102933.

Zhu, H. L., D. A. Pi, W. B. Leng, X. Y. Wang, C. A. A. Hu, Y. Q. Hou, J. L. Xiong, C. W. Wang, Q. Qin, and Y. L. Liu. 2017. Asparagine preserves intestinal barrier function from LPS-induced injury and regulates CRF/CRFR signaling pathway. Innate Immun 23:546–556.